LUNAR SECONDARY CRATERS MEASURED USING LROC IMAGERY: SIZE-VELOCITY DISTRIBUTIONS OF EJECTED FRAGMENTS. [1]Kelsi N. Singer, [1]Bradley L. Jolliff, [1]William B. McKinnon. [1]Department of Earth and Planetary Sciences and McDonnell Center for the Space Sciences, Washington University in St. Louis, MO 63130 (ksinger@levee.wustl.edu).

Introduction: Observations are necessary to validate experiments and modeling of cratering and ejecta physics. Here we map lunar secondary craters and estimate the size and velocity of the ejecta fragments that formed them. We characterize two main aspects of the data: 1) the secondary size fall-off as a function of distance from the primary crater, and 2) the size-velocity distribution (SVD) of ejected fragments. These data can be compared for craters across the Solar System—on the Moon [1-3], terrestrial planets [2,3], icy satellites [4], and small bodies—to examine trends and assess the role of material and dynamical parameters in fragment formation and ejection.

Mapping: With the modern Lunar Reconnaissance Orbiter (LRO) dataset we can explore a range of primary crater sizes and target materials. The LRO Wide Angle Camera (WAC) 100 m/pixel global mosaic served as the base for all mapping. We also examined Narrow Angle Camera (NAC) images (~0.5–1.5 m px^{-1}) for confirmation of secondary crater morphologies. High sun mosaics were useful for following crater rays.

Secondary fields around three primary craters have been mapped to date: Kepler (31 km diameter), Copernicus (93 km) and Orientale (660 km to Outer Rook). Only the craters with the highest likelihood of being secondaries (in obvious radial chains or clusters), and whose diameters were clear, are utilized in the subsequent analysis.

Fragmentation Theory: Near surface material inside the transient cavity is predicted to break up and be ejected directly by stress-wave interference forming spall plates [5,6]. Typical spall plate thickness (l_{spall}) is estimated from the following:

$$l_{spall} = \frac{2a_i T(\delta/\rho)^{1/2}}{\rho C_L \upsilon_{ej}} \propto A\upsilon_{ej}^{-1}, \quad (1)$$

where a_i is the primary impactor radius (estimated by scaling from the crater size [7]) and δ the impactor density. T, C_L, and ρ are the tensile strength, P-wave speed, and density of the target material, respectively (values of 100 MPa [5], 5.3 km s^{-1} [5], and 2500 kg m^{-3} [8] are used). The function predicts spall size is inversely related to the speed at which a given spall plate is ejected (υ_{ej}). For simplicity, in this abstract we assume ρ=δ for asteroidal impactors on the Moon. Spall plates may be up to 10·l_{spall} in their other two dimensions, thus a mean spall diameter is estimated as

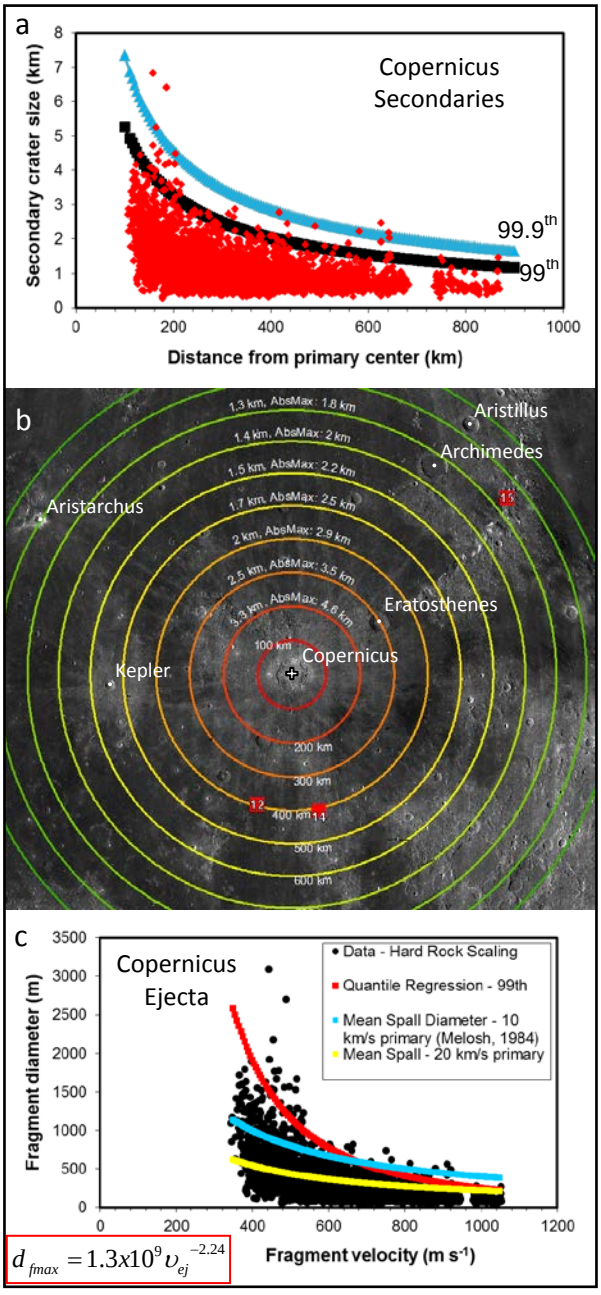

Figure 1. (a) Quantile regression fits to the secondary measurements for the 99th quantile (a typical large secondary) and the 99.9th quantile (absolute max. secondary size). (b) Map of expected secondary sizes at a given distance. Apollo 12, 14, and 15 sites marked with red squares. (c) Size-velocity distribution of estimated ejecta fragments and quantile regression fit to upper envelope (99th quantile, red curve and equation). Also shown are two curves for predicted spall sizes (primary impact speeds of 10 and 20 km s^{-1}).

$100^{1/3} \cdot l_{spall}$. Spall plates are ejected at relatively high velocities, though, and may break up during flight.

Grady-Kipp theory predicts a mean or preferred fragment size for material ejected during the main excavation flow that is smaller than spall for the same conditions (the sizes are proportional to $v_{ej}^{-2/3}$).

Ejecta Fragment Size-velocity Distributions (SVDs): We estimated the velocity and size (d_{fmax}) of the ejecta fragment that formed each secondary crater from the range equation for a ballistic trajectory on a sphere and Schmidt-Holsapple scaling relations (methods as in [4]). Size scaling was carried out in the gravity regime for both non-porous and porous endmember target material properties [9]. Primary transient cavity diameters were estimated according to [10].

Results: A power law function was fit to the upper envelope of the SVDs (Fig. 1c) using quantile regression: $d_{fmax} = A v_{ej}^{-\beta}$. The pre-exponential factor, A, generally scales with primary crater size. The velocity exponent, $-\beta$, is predicted by spallation theory to be -1, and limited to the interval [1,4/3] by coupling parameter scaling (for the specific case when d_{fmax} does not depend on C_L [4]). It is observed, however, to vary between -1 and -3 on both icy and rocky bodies (Fig. 2). Craters less than 40 km in diameter come closest to having a $-\beta$ of -1. Larger craters generally have steeper exponents, but this trend is not consistent.

The Copernicus dataset is the most robust—it has the greatest number of measurements (n = 5,440 certain secondaries) and least contamination from other secondary fields or primary cratering (it is a large, young crater on a largely mare surface). A quantile regression fit to the upper envelope of the derived fragment data (Fig. 1c), yields a pre-exponential factor, A, that is comparable in magnitude to that predicted by spallation theory (Eq. 1). The comparison is better for slower assumed primary impact speeds (10 km s^{-1}). The velocity exponent of -2.2 is similar to that found by [2,3] but shows a steeper fall-off in sizes than predicted by current spallation theory.

Largest Fragments at Escape Velocity. Extrapolating the power-law fits for largest fragment size to the Hill-sphere escape velocity (2.34 km/s) gives fragment sizes of 30, 40 and 860 m for Kepler, Copernicus and Orientale, respectively. These fragments would go into orbit, and may eventually re-impact the Moon, or impact the Earth as meteorites.

Size and location of secondary craters. Secondaries are abundant and quite large even at a substantial distance from Copernicus (Fig. 1a,b). This fact has implications for age dating, as secondaries from various impacts are heterogeneously distributed around the Moon.

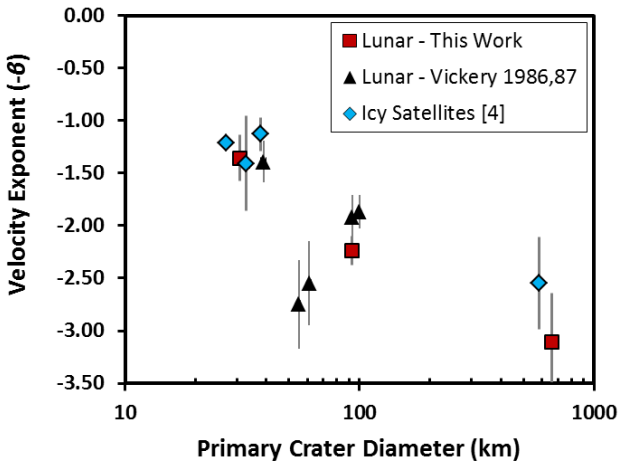

Figure 2. Comparison of velocity exponents ($-\beta$) for primary craters on the Moon and icy satellites [4]. This exponent describes how quickly ejecta fragment sizes decrease with increasing ejection velocity.

Discussion and Conclusions:

- New measurements of secondary craters using LROC images allow characteristics of ejecta distributions as a function of crater size.
- Current spallation theory better predicts the magnitude of fragment sizes for the rocky lunar data than for icy satellite examples [4]. However, there is still a range of velocity exponents that are generally steeper than predicted. Future updates to spallation theory may address this issue.
- Fragmentation and meteorite ejection influence the exchange of material between planets, ejecta transport of material across a planet's surface, and the origin of small craters, which affects our understanding of age determination through crater size-frequency distributions. The size and location of secondaries can be roughly estimated, and potentially factored into any interpretations based on crater counting.
- Fragments as large as ~1 km could be ejected in the largest lunar impacts. More typical sizes are in the 10s of meters for mid-sized impacts.

References: [1] Singer K.N. et al. (2013) *AGU abs.* #P41F-1976. [2] Vickery A.M. (1986) *Icarus 67*, 224-236. [3] Vickery A.M. (1987) *GRL 14*, 726-729. [4] Singer K.N. et al. *Icarus* 226, 865-884, doi:10.1016/j.icarus.2013.06.034. [5] Melosh H.J. (1984) *Icarus 59*, 234-260. [6] Melosh H.J. (1989) Impact Cratering: A Geologic Process. OUP, p. 107. [7] Holsapple K.A. (1993) *AREPS 21*, 333-373. [8] Wieczorek M.A. et al. (2013) *Science 339*, 671-675. [9] Holsapple K.A. (2007) http://keith.aa.washington.edu/crater-data/scaling/theory.pdf. [10] McKinnon W.B. and Schenk P.M. (1985) *LPSC XVI*, 544-545.